Int. J. Electrochem. Sci., 7 **(2012)** 9410 - 9422

International Journal of
ELECTROCHEMICAL
SCIENCE
www.electrochemsci.org

The Role of Cl^- Ions During the Adsorption of Polyethylene Glycol (MW 20,000) onto a Polycrystalline Gold Electrode

Alia Méndez and G. Trejo[*]

Laboratorio de Materiales Compuestos y Recubrimientos Funcionales. Centro de Investigación y Desarrollo Tecnológico en Electroquímica (CIDETEQ). Parque Tecnológico Sanfandila, Pedro Escobedo, A.P. 064, C.P. 76703, Querétaro, México.
[*]E-mail: gtrejo@cideteq.mx

Received: 2 August 2012 / *Accepted:* 14 September 2012 / *Published:* 1 October 2012

The adsorption of polyethylene glycol (MW 20,000) (PEG_{20000}) onto a polycrystalline gold electrode in the presence of Cl^- ions was studied by differential capacitance measurements and quartz crystal microbalance. This study provides new physical insights into the adsorption behavior of this polymer onto a solid electrode in the presence of Cl^- ions and $KClO_4$. Three potential-based behaviors were observed: in the potential range from -0.90 to -0.62 V *vs.* the saturated calomel electrode (SCE), the principal adsorption process was observed to form a condensed PEG_{20000} phase. In addition, there was a slight desorption of PEG_{20000}. In the potential range from -0.62 to -0.10 V *vs.* SCE, the addition of Cl^- ions to the solution reduced the amount of PEG_{20000} adsorbed. This behavior was associated with the lower number of available active adsorption sites on the gold surface due to the adsorption of Cl^- ions. In addition, we observed the superposition of the two adsorption processes on different active sites. PEG was adsorbed on lower-energy adsorption sites (the most accessible adsorption sites), whereas Cl^- ions were adsorbed on higher-energy adsorption sites (the least accessible adsorption sites). The potential range from -0.10 to 0.35 V *vs.* SCE was dominated by the adsorption of Cl^- ions, and a displacement of adsorbed PEG_{20000} molecules associated with the adsorption of Cl^- anions was observed.

Keywords: Additives, adsorption, chloride ions, poly(ethylene glycol), quartz crystal microbalance

1. INTRODUCTION

Organic substances are widely used in metal electrodeposition to improve the properties of electroplated coatings. Polyethylene glycol (PEG) is one of the main components of contemporary acid electrolytes for the electrodeposition of bright copper coatings [1-3] and bright zinc coatings [4]. PEG compounds are commonly used as additives to achieve high throwing power and are also used in electroplating baths to produce super conformal deposition [5]. The role of PEG in controlling the

coating quality is primarily associated with the adsorption of polymer molecules at the electrode surface; these traits require the presence of Cl^- ions as another constituent of the plating bath. Various studies have suggested that in the presence of Cl^-, the adsorption of PEG onto an electrode surface forms a barrier that inhibits metal deposition and increases the overpotential for the discharge of metal ions, such as Zn(II) [6] or Cu(II) [7] ions. Furthermore, the degree of inhibition increases with increasing molecular weight for polyethoxylated compounds [8]. In establishing these relationships, special attention was paid to PEG adsorption. Recently, using capacitance measurements, Petri et al. [9] established that PEG molecules adsorb onto an Au(111) electrode to form two-dimensional condensates. Using *in situ* spectroscopic ellipsometry, Walker et al. [10] demonstrated that PEG is only weakly adsorbed onto a Ru electrode in the absence of Cl^- ions. In addition, in situ electrochemical scanning tunneling microscopy (EC-STM) of PEG (MW 1,000) (PEG_{1000}) molecules adsorbed onto a Fe(110) surface [11] revealed that PEG_{1000} exhibits a well-ordered structure on this surface. On the basis of this finding, Kim et al. [11] proposed a model for PEG adsorption in which PEG_{1000} is adsorbed in a planar configuration via the oxygen atoms.

Based on Raman spectroscopy data, Healy et al. [12,13] suggested that the type of PEG species adsorbed onto an electrode surface depends on the applied potential. Specifically, these authors proposed that neutral PEG molecules are adsorbed at more negative potentials, at which copper deposition occurs. However, at potentials close to the open-circuit potential, PEG adsorbs as a copper chloride complex with the polymer acting as a ligand, analogous to a crown ether. In addition, differential capacitance measurements in a PEG-containing H_2SO_4 electrolyte solution exposed to a copper substrate revealed that PEG was weakly adsorbed onto the copper surface [14]. Using a quartz crystal microbalance (QCM) and electrochemical impedance spectroscopy, Kelly and West [15,16] observed that the addition of PEG alone to an electrolytic bath had only a small effect on the electrode kinetics and that Cl^- ions alone promoted the copper deposition reaction. However, they also reported that when both PEG and Cl^- ions were present in the solution, the PEG monolayer collapsed into spherical aggregates.

The simultaneous presence of PEG and Cl^- ions as additives produces specific effects on metal ion reduction. It is now known that these effects are related to the capacity of these additives to be absorbed onto the electrode surface. Previously [17,18], we used the thermodynamic method of Lipkowski et al. [19-21], who investigated the adsorption of organic molecules onto solid electrodes, to investigate the adsorption of PEG_{20000} and Cl^- ions onto polycrystalline Au in a $KClO_4$ solution and to quantify the thermodynamic parameters of the adsorption, namely, the surface tension, the relative Gibbs surface excess, and the Gibbs energy of adsorption. In the present work, we used a quartz crystal microbalance (QCM) and differential capacitance measurements to investigate the role of Cl^- ions during the adsorption of PEG (MW 20,000) onto a polycrystalline gold electrode.

2. EXPERIMENTAL

The following solutions were used in the study of PEG_{20000} adsorption: S_0 (0.1 M $KClO_4$), S_1 (=S_0+ 12.3 mM KCl), S_2 (=S_0+5 μM PEG_{20000}), and S_3 (=S_1+5 μM PEG_{20000}). The concentration of

KCl was selected to maintain a [PEG_{20000}]/[KCl] concentration ratio of 4×10^{-4}. This ratio is similar to that employed for the electrodeposition of a Zn-Mn alloy [4]. A stock solution of 5 mM PEG_{20000} was prepared by dissolving PEG_{20000} in 0.1 M $KClO_4$, and another 1.0 M stock solution of KCl was prepared by dissolving KCl in 0.1 M $KClO_4$. The solutions were prepared with ultra-pure water (18 $M\Omega cm^{-1}$) and analytical-grade reagents (Sigma-Aldrich, in the highest purity available) immediately before each electrochemical experiment. Before each electrochemical experiment, the solution was deoxygenated for 30 min with ultra-pure nitrogen (Praxair), and the experiments were performed under a nitrogen atmosphere at 25.0 ± 0.5 °C.

The experiments were performed in a conventional three-electrode cell with a water jacket. A potentiostat/galvanostat (Autolab, model PGSTAT 30) and a QCM (Maxtek, model 710), controlled by independent computers, were used to simultaneously measure the electrochemical parameters and the frequency of the quartz crystal. An AT-cut quartz crystal with a nominal frequency (f_0) of 5 MHz, which was covered on both sides with an Au film (Maxtek, CA), was used as the working electrode (Au-QCM). The geometric area of the Au-QCM electrode was 1.37 cm^2. The real area of the electrode was 2.98 cm^2, as determined according to the method described by Woods [22]; the surface roughness factor, R_f, was 2.17. All results reported in this work refer to the real area. A saturated calomel electrode (SCE) and a graphite rod were used as the reference and counter electrodes, respectively. To minimize iR-drop effects, the reference-electrode and working-electrode compartments were connected with a Luggin capillary.

The QCM signal was recorded as Δf, where $\Delta f = f - f_{initial}$, as a function of time and of electrode potential. The experimental frequency change was expressed as follows [23,24]:

$$\Delta f = -C_f \Delta m + \Delta f_\eta + \Delta f_r + ... \qquad \text{(Eq.1)}$$

Where the first term on the right-hand side of Eq. (1) is the Sauerbrey term [25], which represents the total mass change at the electrode surface. Other possible contributions to the frequency change include changes in the solution viscosity (Δf_η) [26] and the surface roughness (Δf_r) [27]. Prior experimental studies have shown that surface roughness can drastically affect the resonance frequency. This effect was attributed to relatively rough surfaces, which trap a larger quantity of solvent molecules in surface cavities than smoother surfaces [28-31]. In the present work, polished Au-QCM electrodes (with a roughness of 12 nm, as measured by atomic force microscopy (AFM)) were used to minimize the effects of surface roughness, and the effects of viscosity variations were expected to be negligible. Prior to the measurements, the sensitivity factor (C_f = 0.049 Hz cm^2 ng^{-1}*R_f) of the quartz crystal was determined using the chronoamperometry calibration method described by Vatankhah et al. [32].

Each experiment was performed at least five times; the accuracy of the charge density (Q) values was ± 0.15 μC cm^{-2} and of the mass change (Δm) was ± 0.57 ng cm^{-2}.

3. RESULTS AND DISCUSSION

3.1. Characterization of the electrode surface by cyclic voltammetry

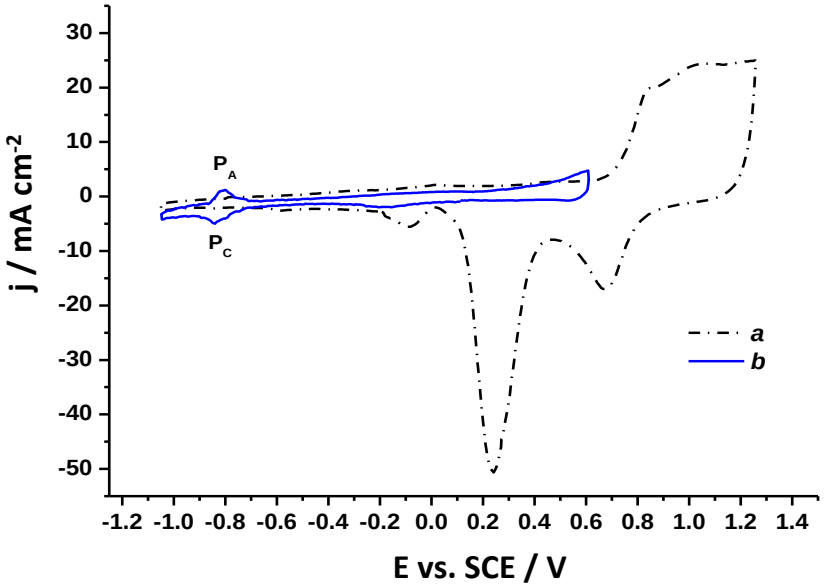

Figure 1. Cyclic voltammograms for a polycrystalline gold electrode in solutions (a) S_0 (0.1 M KCl) and (b) S_0 + 5 μM PEG_{20000}. Potential range, -1.18 to 1.2 V *vs.* SCE; scan rate, 0.05 V s^{-1}.

Prior to each experiment, the Au-QCM electrode was activated in 0.5 M H_2SO_4 by cycling the potential between the onset potentials of hydrogen and oxygen evolution at 0.1 Vs^{-1} until no changes were observed in the voltammogram (~10 cycles). The Au-QCM electrode was then transferred to a cell containing the supporting electrolyte (solution S_0; 0.1 M $KClO_4$), in which the Au-QCM electrode was again activated by cycling the potential between the onset potentials of hydrogen and oxygen evolution at 0.1 Vs^{-1} until no changes were observed in the voltammogram (~four cycles). Figure 1 (curve a) shows a typical voltammogram obtained for an Au-QCM electrode in solution S_0. The observed behavior was similar to that reported by Stolberg et al. [33] for an Au electrode in a $KClO_4$ solution. Specifically, for potentials more positive than 0.7 V *vs*. SCE, oxidation of the gold surface was observed. The cathodic current density peaks at approximately 0.75 and 0.20 V *vs*. SCE correspond to the reduction of gold oxides formed during the anodic sweep. This behavior was considered an indication of a clean, active Au-QCM surface.

When PEG_{20000} was added to solution S_0 at a concentration of 5 μM, the shape of the voltammogram in the double-layer region changed significantly (Fig. 1, curve b). The j-E profile displayed a pair of broad current peaks in the anodic (P_A; approximately -0.80 V *vs*. SCE) and cathodic (P_C; approximately -0.85 V *vs*. SCE) scans, both of which were associated with the adsorption-desorption of PEG_{20000}. The onset of an increase in the anodic current density at approximately 0.6 V *vs*. SCE was caused by the oxidative decomposition of PEG_{20000}. Thus, in the presence of PEG_{20000}, the double-layer region is limited by the faradic current density of hydrogen evolution on the negative side and by the oxidation of PEG_{20000} on the Au-QCM surface on the positive side.

3.2. Voltammetric and QCM studies

To determine the effect of the adsorption of PEG_{20000} and Cl^- ions on an Au-QCM electrode, we performed simultaneous voltammetric and QCM studies in the potential range –1.0 to 0.6 V *vs.* SCE using the following solutions: S_0 (0.1 M $KClO_4$; curve a), S_1 (S_0 + 12.3 mM KCl; curve b), S_2 (S_0 + 50 μM PEG_{20000}; curve c), and S_3 (S_1 + 50 μM PEG_{20000}; curve d). The potential scans were initiated in the negative direction from the open-circuit potential (E_{OCP}), with a potential scan rate (v) of 0.05 V s^{-1}.

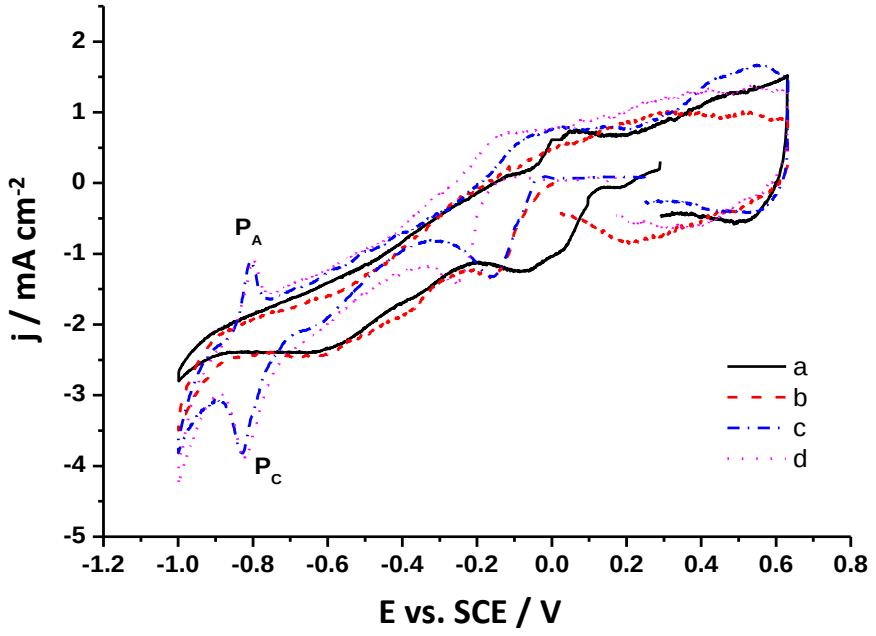

Figure 2. Cyclic voltammograms recorded for solutions (a) S_0 (0.1 M $KClO_4$), (b) S_1 (S_0 + 12.3 mM KCl), (c) S_2 (S_0+5 μM PEG_{20000}), and (d) S_3 (S_1+5 μM PEG_{20000}). Potential range, -1.0 to 0.6 V *vs.* SCE; scan rate, 0.05 V s^{-1}.

Figure 2 shows the voltammograms obtained. The profile obtained for the supporting electrolyte (solution S_0; curve a) presents the characteristic behavior of an Au electrode free of impurities in a $KClO_4$ [33] solution. Similar behavior was observed in the presence of Cl^- ions (solution S_1; curve b). In Figure 2, curve c corresponds to the cyclic voltammogram obtained in the presence of PEG_{20000}, in which the formation of the peaks P_A and P_C is observed and is associated with the adsorption-desorption processes of the species [17,34]. In contrast, the addition of Cl^- ions to the $KClO_4$/PEG_{20000} system (solution S_3; curve d) did not significantly modify the shape of the voltammogram or the intensity of the current density in the P_A and P_C peaks. Therefore, the adsorption-desorption mechanism of PEG_{20000}, which corresponds to the processes P_A and P_C, is independent of the presence of Cl^- ions in the dissolution.

To verify the adsorption of PEG_{20000} and Cl^- ions in the potential range –1.0 to 0.6 V *vs.* SCE, based on the frequency changes recorded by QCM, we constructed graphs of $d\Delta m\ dt^{-1}$ *vs. E*, known as massograms [35] (Fig. 3), in which $d\Delta m\ dt^{-1}$ is the rate of mass change (mass flux) that occurs at the electrode surface. For mass changes that are associated with charge-transfer processes at the electrode

surface (faradaic processes), $d\Delta m\ dt^{-1}$ is directly proportional to the current density; hence, a massogram is analogous to a voltammogram. In a massogram, a negative mass flux corresponds to a mass loss (desorption), and a positive mass flux corresponds to a mass gain (adsorption).

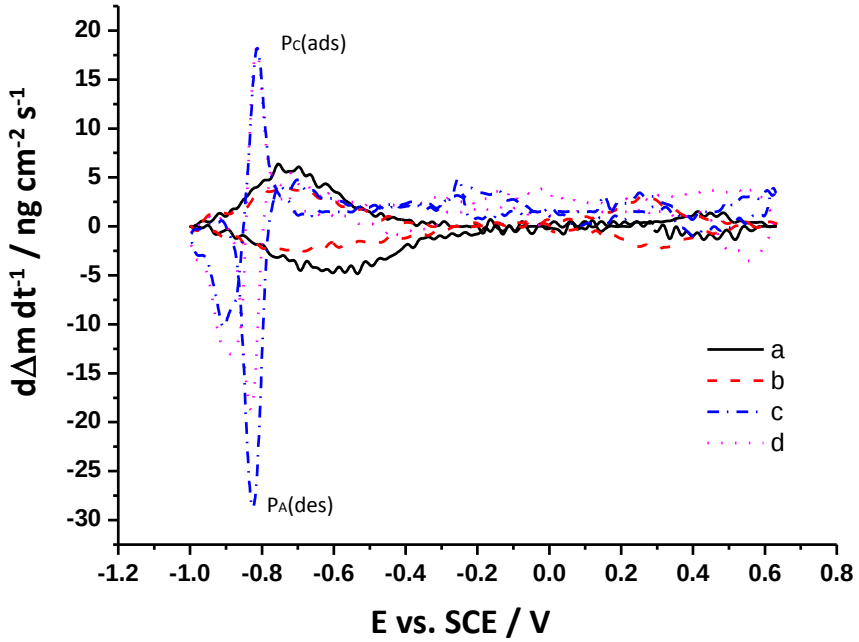

Figure 3. Series of massograms for an Au-QCM electrode obtained simultaneously with the cyclic voltammograms in Fig. 2 for solutions (a) S_0 (0.1 M $KClO_4$), (b) S_1 (S_0+ 12.3 mM KCl), (c) S_2 (S_0+5 μM PEG_{20000}), and (d) S_3 (S_1+5 μM PEG_{20000}).

When PEG_{20000} or the PEG_{20000}/Cl^- mixture were present in the dissolution (Fig. 3; curves c and d, respectively), a positive mass flux peak (mass gain) at approximately -0.8 V *vs.* SCE was observed during the potential sweep in the negative direction ($P_{C(ads)}$ peak). This potential value is similar to that obtained for the reduction process, P_C, observed by cyclic voltammetry (Fig. 2). It is important to note that the mass flux density in the $P_{C(ads)}$ peak is independent of the presence of Cl^- ions. This result implies that the adsorption velocity of the polymer is not affected by the presence of Cl^- ions at the interface. In addition, during the potential sweep in the positive direction, a negative mass flux peak (mass loss, $P_{A(des)}$ peak) was observed at approximately -0.85 V *vs.* SCE, which decreased in intensity in the presence of Cl^- ions. Therefore, the velocity of PEG_{20000} desorption from the electrode surface decreases in the presence of Cl^- ions. In addition, the potential value (= -0.85 V *vs.* SCE) was similar to that obtained for the P_A peak during the voltammetric study. The adsorption of PEG_{20000} in the presence of Cl^- ions was further characterized by differential capacitance measurements, and the results obtained are described in the following section.

3.3. Differential capacitance and QCM measurements

In this study we performed simultaneous measurements of differential capacitance and of change of mass (using QCM) onto electrode surface, in the potential range –1.0 to 0.7 V *vs.* SCE using

the following solutions: S_0 (0.1 M $KClO_4$; curve a), S_1 (S_0 + 12.3 mM KCl; curve b), S_2 (S_0 + 50 μM PEG_{20000}; curve c), and S_3 (S_1 + 50 μM PEG_{20000}; curve d).

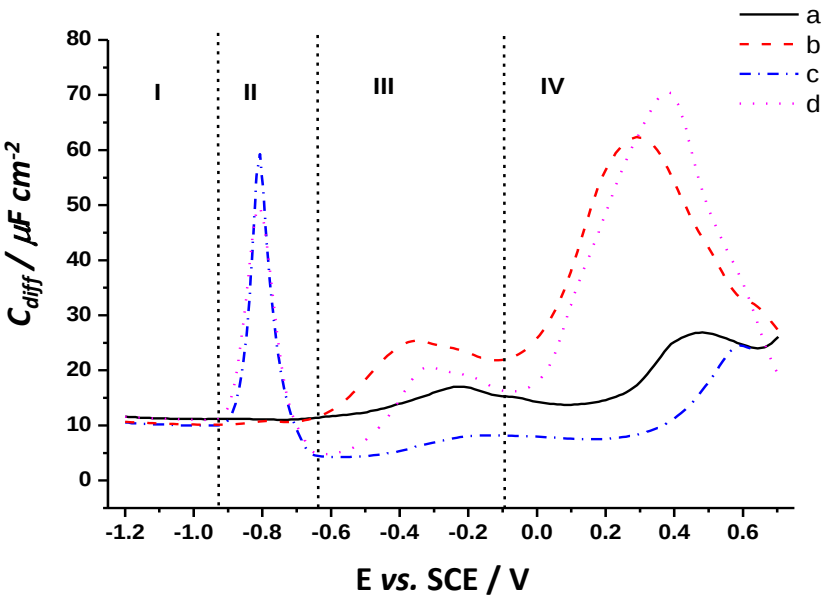

Figure 4. Differential capacitance ($C_{diff.}$) *vs.* potential (E) curves obtained for the polycrystalline Au-QCM electrode obtained in solutions (a) S_0 (0.1 M $KClO_4$), (b) S_1 (S_0+ 12.3 mM KCl), (c) S_2 (S_0+5 μM PEG_{20000}), and (d) S_3 (S_1+5 μM PEG_{20000}). Scan rate, 0.005 V vs. SCE; AC modulation frequency, 25 Hz.

Immediately after adding PEG_{20000}, Cl^- ions or PEG_{20000} + Cl^- ions to solution S_0 at the open-circuit potential (E_{OCP}), a potential value *E* (= -1.18 V *vs.* SCE) was imposed on the Au-QCM electrode. Using this potential as a starting point, a potential scan was initiated in the positive direction. Figure 4 shows the typical $C_{diff.}$ *vs. E* curves obtained from the following solutions: S_0 (curve a), S_1 (curve b), S_2 (curve c), and S_3 (curve d). Four potential regions are clearly observed: region I, from -1.18 to -0.92 V *vs.* SCE; region II, from -0.92 to -0.62 V *vs.* SCE; region III, from -0.62 to -0.10 V *vs.* SCE; and region IV, from -0.10 to 0.7 V *vs.* SCE.

In region I, all curves coincide, which indicates that neither PEG_{20000} nor the Cl^- ions are adsorbed on the electrode surface in this potential range. The $C_{diff.}$ *vs. E* curve that was obtained in the presence of Cl^- ions (solution S_1;curve b) represents the typical behavior for the adsorption of Cl^- ions on an Au(221) surface [36]. Specifically, two capacitive peaks associated with the adsorption of Cl^- ions on an Au surface were observed. The first peak was observed in the potential interval from -0.62 to -0.10 V *vs.* SCE (corresponding to region III); the second peak was observed in the interval from -0.10 to 0.70 V *vs.* SCE (region IV) and was larger than the first peak. Adsorption is, in general, localized on solid surfaces; therefore, the peaks in the $C_{diff.}$ *vs. E* curves correspond to the adsorption of the Cl^- ions onto active sites with different energy levels. The most accessible adsorption sites, whether due to their energy or their steric orientation, correspond to the most cathodic peak. Conversely, the least accessible adsorption sites correspond to the most anodic peak [36].

When only PEG_{20000} was present (solution S_2; curve c), a pseudo-capacitive peak appeared in the interval from -0.92 to -0.62 V *vs.* SCE (region II). This peak is characteristic of the adsorption–desorption processes of neutral organic macromolecules [37]. However, according to Miller and Grahame [38-40], this peak can be caused by some segments of the adsorbed macromolecules that were not desorbed during the desorption process. In addition, in the potential range from -0.62 to -0.45 V *vs.* SCE (region III), the capacitance values reached a plateau, which suggests that two-dimensional condensation occurred [9].

The curve with PEG_{20000} and Cl^- ions (solution S_3; curve d) exhibited a pseudo-capacitive peak in the interval from -0.92 to -0.62 V *vs.* SCE (region II), corresponding to the desorption–adsorption processes of PEG_{20000}. The intensity of this peak was less than that of the peak observed solely in the presence of PEG_{20000} (solution S_2; curve c). Likewise, the value of the peak potential was independent of the presence of Cl^- ions in the solution, which indicates that the activity of the supporting electrolyte is not affected by the presence of Cl^- ions. In region III, in the interval from -0.62 to -0.58 V *vs.* SCE, the capacitance was essentially the same as that obtained with the S_2 solution, which suggests that two-dimensional condensation occurred. The formation of a condensed film can be observed as a characteristic decrease in the double-layer capacitance, which leads to a so-called capacity pit. Molecules with alkyl-ether oxygen atoms are known to adsorb onto metal surfaces and form two-dimensional condensates [9].

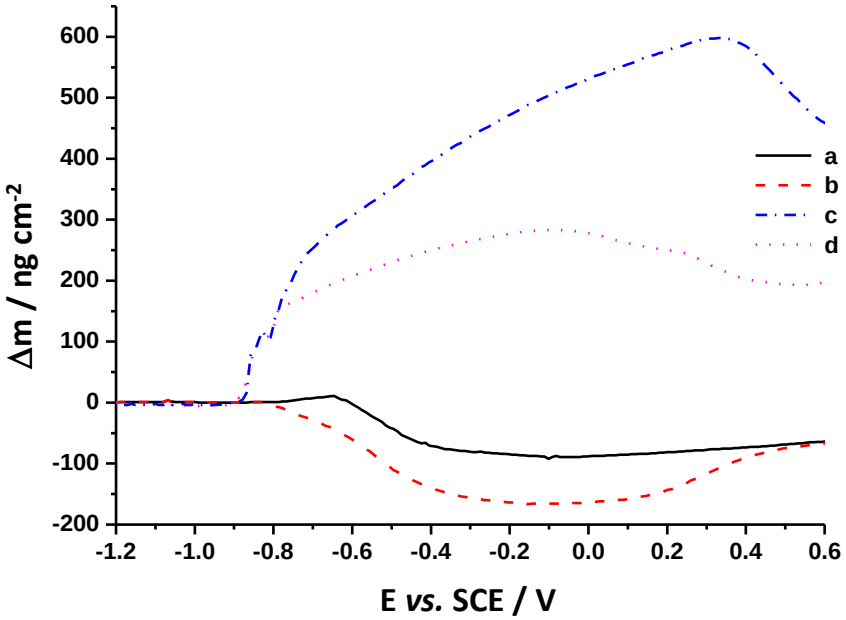

Figure 5. Mass change (Δm) as a function of potential, obtained simultaneously with the differential capacitance ($C_{diff.}$) *vs.* potential (E) curves in Fig. 4 for solutions (a) S_0 (0.1 M $KClO_4$), (b) S_1 (S_0+ 12.3 mM KCl), (c) S_2 (S_0+5 μM PEG_{20000}), and (d) S_3 (S_1+5 μM PEG_{20000}).

At less-negative potentials, i.e., within the interval from -0.58 to -0.10 V *vs.* SCE, capacitance increased due to the adsorption of Cl^- ions; however, the capacitance was still less than that obtained in the presence of Cl^- ions alone (solution S_1; curve b). This behavior is associated with the co-adsorption

of both PEG_{20000} and Cl^- ions. In region IV, the pseudo-capacitive peak obtained in the presence of PEG_{20000} and Cl^- ions exhibited a greater intensity than that obtained in the presence of Cl^- ions alone, indicating a greater influence of the Cl^- ions in this potential region in the presence of PEG_{20000}.

The results shown in Fig. 4 suggest that the adsorption of both PEG_{20000} and Cl^- ions occurs on active adsorption sites of different energies.

Figure 5 presents plots of Δm *vs.* E corresponding to the $C_{diff.}$ *vs*. *E* curves shown in Fig. 4. The Δm values were calculated using Equation 1 and the measurements of the frequency change (Δf). The plots of Δm *vs*. E exhibit the following characteristics:

a) In the interval from -1.18 to -0.92 V *vs*. SCE, the values of superficial mass change are null for all of the considered systems, indicating that in this potential interval, there are no adsorbed species on the Au-QCM electrode surface. This result is in accord with that obtained from the $C_{diff.}$ *vs*. *E* curves (see Fig. 4).

b) A loss of superficial mass was observed at more positive potentials in the presence of ClO_4^- ions (solution S_0; curve a) or in the presence of Cl^- ions (solution S_1; curve b). This effect is attributed to changes in the interface structure due to the presence of the anions [14].

c) The Δm *vs*. E graph obtained from solution S_2 (S_0 + 5 μM PEG_{20000}) (curve c) exhibited a constant increase in mass change (adsorption) in the interval from -0.90 to 0.40 V *vs*. SCE. At potentials more positive than 0.40 V *vs*. SCE, the amount of mass decreased, indicating a superficial desorption associated with the oxidation of the adsorbed PEG_{20000} species [42,43].

d) In the potential range -0.90 to -0.77 V *vs*. SCE, the curve obtained from solution S_3 (S_1 + 50 μM PEG_{20000}) (curve d) presents a similar increase in mass to that obtained from the S_2 solution. At potentials higher than -0.77 V *vs*. SCE, the adsorbed mass of PEG_{20000} and Cl^- ions was lower than that obtained in the presence of PEG_{20000} alone (solution 2) in the same potential interval. From the results presented in the $C_{diff.}$ *vs*. E graph (see Fig. 4), is possible indicate that this behavior is associated with the co-adsorption of both PEG_{20000} and Cl^- ions and with a decrease in the number of sites available for the adsorption of PEG_{20000} due to the adsorption of Cl^- ions.

In addition, it is important to note that a decrease in the superficial mass was observed at E = -0.8 V *vs*. SCE, which is indicative of a desorption process. This potential value (E = -0.8 V *vs*. SCE) is similar to that at which the peaks P_A and $P_{A(des)}$ occur in the voltammograms and massograms and to the potential value of the pseudo-capacitive peak observed in the $C_{diff.}$ *vs*. E curves. Therefore, we propose that this behavior corresponds to the partial desorption of PEG_{20000} from the Au-QCM electrode surface.

3.4. Study of the adsorption by QCM at various potential adsorption values (E_i)

To verify the adsorption of PEG_{20000} and Cl^- ions onto the polycrystalline Au-QCM electrode surface in each potential region (see the $C_{diff.}$ *vs. E* graphs), measurements of the mass change on the electrode surface at different adsorption potentials *(E_i)* were performed with a QCM. This study was performed according to the following procedure.

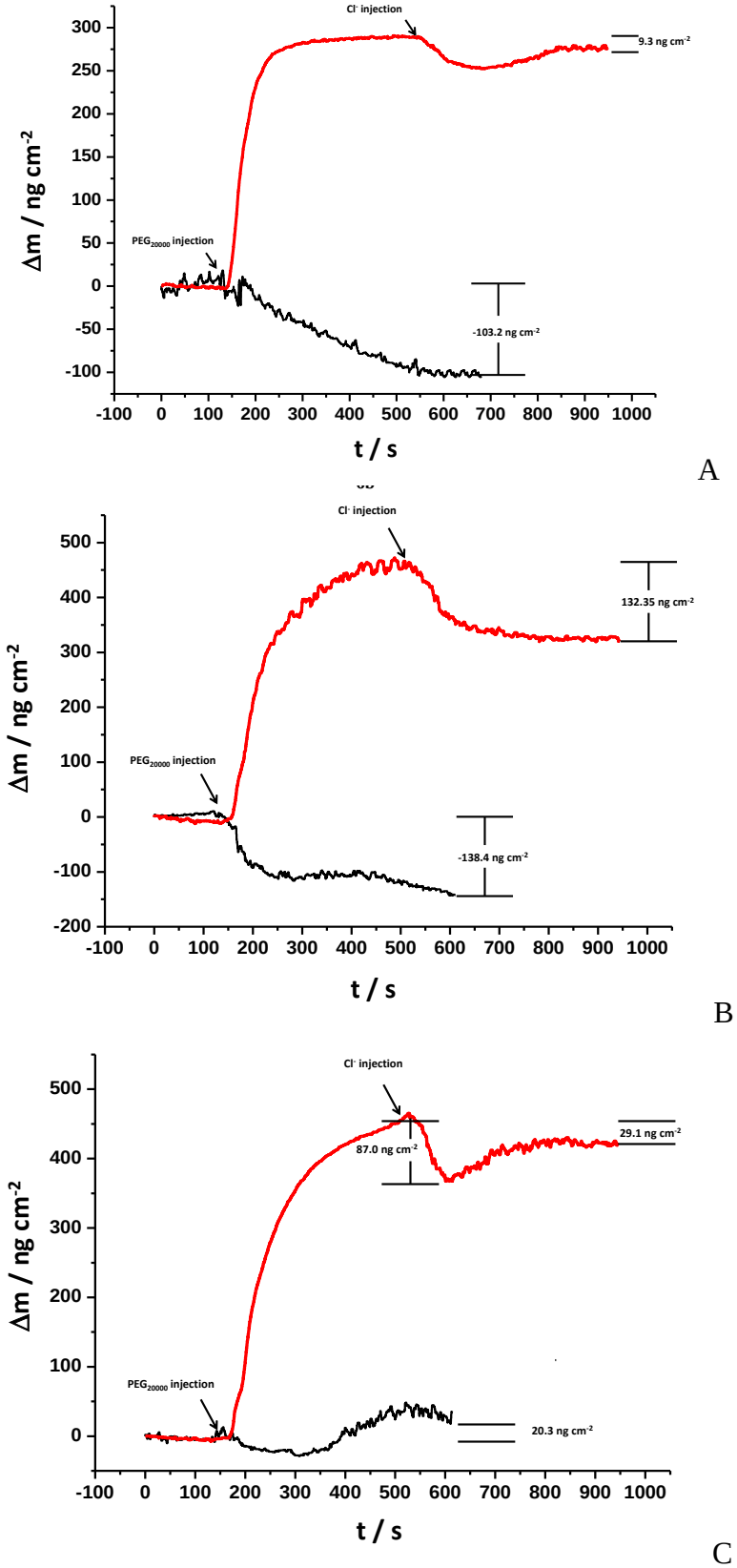

Figure 6. Mass change (Δm) as a function of time after adding PEG_{20000} and Cl^- ions to solution S_0 (0.1 M $KClO_4$) to a final concentration of 5 μM PEG_{20000} + 12.3 mM KCl. The experiments were each performed at a constant electrode potential (E_i): (a) -0.68, (b) -0.35, and (c) 0.29 V *vs.* SCE.

After a typical voltammogram for an Au-QCM polycrystalline electrode in a S_0 solution was obtained (see Section 3.1), an adsorption potential value E_i was imposed on the electrode. After the frequency of the microbalance had remained stable ($\Delta f \approx 0$) for 150 s in the electrolytic S_0 solution (with constant agitation) at E_i, a PEG_{20000} stock solution was injected to yield a solution concentration of 5 μM PEG_{20000}. The change in the resonance frequency of the quartz crystal was then recorded for 7 min to monitor the adsorption of PEG_{20000}; agitation was continued throughout this 7-min period. Immediately afterward, sufficient KCl was added to obtain a 12.3 mM concentration of Cl^- ions in the solution, and the adsorption of Cl^- ions was monitored for an additional 7 min.

Figure 6 shows typical Δm *vs.* t (Δm was calculated using Eq. (1)) plots obtained at three potential values for adsorption (E_i): -0.68 (Fig. 6a), -0.35 (Fig. 6b), and 0.29 V *vs.* SCE (Fig. 6c). These potentials correspond to regions II, III, and IV in the $C_{diff.}$ *vs.* E curves (Fig. 4). The behavior exhibited in the graphs reveals the following characteristics: immediately after the addition of PEG_{20000}, the mass on the electrode surface increased rapidly, reaching a stationary state after 7 min; this behavior is characteristic of PEG_{20000} adsorption onto an Au-QCM [17] surface. However, when the Cl^- ions were added, the adsorption behavior depended on the imposed potential (E_i).

Specifically, when the imposed adsorption potential was -0.68 V *vs.* SCE (Fig. 6a), the addition of the Cl^- ions to the solution caused a decrease in the adsorbed mass. This behavior is associated with the alteration of the double-layer structure due to the presence of the Cl^- ions, followed by the observed competition between the formation of the condensed phase of adsorbed PEG_{20000} and the adsorption of Cl^- ions. Due to the negative polarization of the surface electrode in this potential region, the Cl^- ions are repelled to the diffuse double layer, and the formation of the condensed phase of PEG_{20000} is re-established. Consequently, the value of the adsorbed mass returns to a value similar to that obtained before the addition of the Cl^- ions. In addition, Figure 6a presents the curve obtained when PEG_{20000} is absent, in which the observed loss of mass in the electrode surface is associated with the alteration of the double-layer structure due to the presence of Cl^- ions.

When the adsorption potential was -0.35 V *vs.* SCE (Fig. 6b), which corresponds to region III of the capacitance curves (Fig. 4), a loss of mass was observed immediately after the addition of the Cl^- ions, followed by the presence of a stationary state. This result indicates that an adsorptive equilibrium was reached. The amount desorbed due to the presence of Cl^- ions in the interphase was similar, even when the sub-monolayer of PEG_{20000} was formed. This result indicates the co-adsorption of PEG_{20000} and Cl^- ions on the Au surface, given that the adsorption of these two species is selective for different available sites, each with a specific energy level [44]. Therefore, the observed loss of mass corresponds to the displacement of the ClO_4^- ions from the electrode surface due to the adsorption of the Cl^- ions.

When the adsorption potential was 0.29 V *vs.* SCE (Fig. 6c), which corresponds to region IV of the capacitance curves (Fig. 4), the mass of PEG_{20000} desorbed by the addition of Cl^- ions to the solution was greater than that obtained in a solution without PEG_{20000} (solution S_1). This result indicates that the interaction between the substrate and the Cl^- ions at these potentials is sufficiently strong to provoke a displacement of the PEG_{20000} molecules adsorbed on the surface. Subsequently, an increase in the adsorbed mass was observed; this increase was associated with the adsorption of Cl^- ions onto the surface of the Au-QCM electrode.

4. CONCLUSIONS

The present study examined the adsorption of PEG_{20000} onto an Au electrode in the presence of Cl^- ions through the analysis of quantitative data obtained from a quartz crystal microbalance and differential capacitance. The results obtained demonstrated that the adsorption of PEG_{20000} principally occurs in the interval from -0.90 to -0.62 V *vs.* SCE, thus forming a condensed film in two dimensions. In addition, a slight desorption of PEG_{20000} was also observed, and this desorption rate decreased in the presence of Cl^- ions.

Likewise, within the interval from -0.62 to -0.1 V *vs.* SCE, the presence of Cl^- ions in the solution did not result in a greater adsorption of PEG_{20000}; instead, an independent superposition of both adsorption processes occurred on the Au surface. This result is similar to that reported by Petri et al. [9], who used capacity–potential curves in their study of the adsorption of PEG onto Au (111) when Cl^- ions were present. Additionally, the adsorption of both PEG_{20000} and Cl^- ions occurs at active sites of different energies. Specifically, PEG_{20000} adsorbs onto lower-energy sites (those with easier access), whereas the Cl^- ions absorb onto higher-energy sites (those with more difficult access). In the potential interval from -0.1 to 0.35 V *vs.* SCE, a decrease in the adsorbed mass was observed. This decrease was associated with the displacement of adsorbed PEG_{20000} molecules from the surface of the electrode due to the adsorption of Cl^- ions in this region.

ACKNOWLEDGEMENTS
The authors are grateful for financial assistance provided by CONACyT, projects 48440-Y, 48335-Y and 128551. Alia Méndez is grateful to CONACyT for scholarship support.

References

1. J.P. Healy, D. Pletcher, M. Goodenough, *J. Electroanal. Chem*., 338 (1992) 155.
2. L. Bonou, M. Ayraud, R. Denoyel, Y. Massiani, *Electrochim. Acta*, 47 (2002) 4139.
3. J.J. Kelly and A.C. West, *J. Electrochem. Soc*., 145 (1998) 3472.
4. Z.I. Ortíz, P. Díaz-Arista, Y. Meas, R. Ortega-Borges, G. Trejo, *Corrosion Sci*., 51 (2009) 2703.
5. J.D. Reid and A.P. David, *Plat. Surf. Finish*., 74 (January, 1987) 66.
6. T. Akiyama, S. Kobayashi, J. Ki, T. Ohgai, H. Fukushima, *J. Appl. Electrochem*., 30 (2000) 817.
7. D. Stoychev, Trans IMF, 76 (1998) 73.
8. G. Trejo, H. Ruiz, R. Ortega-Borges, Y. Meas, *J. Appl. Electrochem*., 31 (2001) 685.
9. M. Petri, D. M. Kolb, U. Memmert, H. Meyer, *J. Electrochem. Soc*., 151 (2004) C793.
10. M.L. Walker, L.J. Richter, D. Josell, T.D. Moffat, *J. Electrochem. Soc*., 153 (2006) C235.
11. J.W. Kim, J. Y. Lee, S. M. Park, *Langmuir*, 20 (2004) 459.
12. J. Healy, D. Pletcher, M. Goodenough, *J. Electroanal. Chem*., 338 (1992) 155.
13. J. Healy, D. Pletcher, M. Goodenough, *J. Electroanal. Chem*., 338 (1992) 167.
14. D. Stoychev, I. Vitanova, S. Rashkov, T. Vitanov, *Surf. Technol*., 7 (1978) 427.
15. J.J. Kelly and A. West, *J. Electrochem. Soc*., 145 (1998) 3472.
16. J.J. Kelly and A. West, *J. Electrochem. Soc*., 145 (1998) 3477.
17. Alia Méndez, L.E. Moron, L. Ortiz-Frade, Y. Meas, R. Ortega-Borges, G. Trejo, *J. Electrochem. Soc.*, 158 (2011) F45.
18. Alia Méndez, Y. Meas, R. Ortega-Borges, G. Trejo, *J. Electrochem. Soc*., 159 (2012) F48.

19. J. Lipkowski and L. Stolberg in Adsorption of molecules at metal electrodes, J. Lipkowski, P.R. Ross, Eds., p. 171, John Wiley and Sons, New York (1992).
20. L. Stolberg, J. Richer, L. Lipkoswki, D.E. Irish, *J. Electroanal. Chem*., 207 (1986) 213.
21. A.Iannelli, J. Richer, L. Stolberg, J. Lipkowski, *Plat. Surf. Finish*.,77 (July 1990) 47.
22. R. Woods in "Chemisorption at electrodes"; Electroanalytical Chemistry, Vol. 9, A.J. Bard, Editor, p. 119, Marcel Dekker, New York (1997).
23. S. Langerock and L. Heerman, *J. Electrochem. Soc*., 151 (2004) C155.
24. V. Tsionsky, L. Daikhin, E. Gileadi, *J. Electrochem. Soc*., 143 (1996) 2240.
25. G. Sauerbrey, *Z. Phys*., 155 (1959) 206.
26. K.K. Kanazawa and J.G. Gordon, *Anal. Chim. Acta*, 175 (1985) 99.
27. M. Urbakh and L. Daikhin, *Langmuir*, 10 (1994) 2836.
28. L. Daikhin and M. Urbakh, *Faraday Discuss*., 107 (1997) 27.
29. M. Yang, M. Thompson, W.C. Duncan-Hewih, *Langmuir*, 9 (1993) 802.
30. R. Schumacher, J.G. Gordon, O. Melroy, *J. Electroanal. Chem*., 216 (1987) 127.
31. R. Schumacher, G. Borges, K.K. Kanasawa, *Surf. Sci*., 163 (1985) L621.
32. G. Vatankhah, J. Lessard, G. Jerkiewicz, A. Zolfaghari, B.E. Conway, *Electrochim. Acta*, 48 (2003) 1619.
33. L. Stolberg, J. Richer, J. Lipkowski, *J. Electroanal. Chem*., 207 (1986) 213.
34. L. Hong-Qiang, S. G. Roscoe, J. Lipkowski, *J. Sol. Chem*., 29-10 (2000) 987.
35. G. A. Snook, A.M. Bond, S. Fletcher, *J. Electroanal. Chem*., 526 (2002) 1.
36. A.Hamelin and J.P. Bellier, *J. Electroanal. Chem*., 41 (1973) 179.
37. B.B. Damaskin, O.A. Petrii, V.V. Batrakov, Adsorption of Organic compounds on electrodes, Plenum Press, New York (1971).
38. I.R. Miller and D.C. Grahame, *J. Am. Chem. Soc*., 78 (1956) 3577.
39. I.R. Miller and D.C. Grahame, *J. Am. Chem. Soc*., 79 (1957) 3006.
40. I.R. Miller and D.C. Grahame, *J. Colloid Sci*., 6 (1961) 23.
41. F. Szabadvary, K. A. Gschneider Jr., L. Eyring (Eds.), Handbook on the Physics and Chemistry of Rare Earths, Vol. 28, Elsevier, *Amsterdam* (1982), p. 336.
42. E. Bahena., P. F. Méndez., Y. Meas., L. Salgado., R. Ortega., G. Trejo, *Electrochim. Acta*, 49 (2004) 989.
43. A.Méndez, P. Díaz-Arista, L. Salgado, Y. Meas, G. Trejo., *Int. J. Electrochem. Sci*., 3 (2008) 918.
44. Z. Shi and J. Lipkwoski, *J. Electroanal. Chem*., 403 (1996) 225.